

Evaluation of the Floater N219 Structure with CEVL Material in Response to Random Wave Excitation

Windha Umi Alifia^{1,*}, Aries Sulisetyono¹, Bimo Hadi Putro¹

¹ Department of Naval Architecture, Faculty of Marine Technology, Institut Teknologi Sepuluh Nopember, Surabaya, Indonesia

* Corresponding author: windha.alifia@its.ac.id

Abstract. Amphibious aircraft are seaplanes fitted with dual floats attached to the fuselage, allowing for landing and take-offs on aquatic surfaces. This research presents a method for evaluating the structural integrity of amphibious aircraft subjected to stochastic wave load stimulation through a probabilistic framework. The wave loads on the aircraft are assessed using the panel approach in a time domain simulation with ANSYS AQWA. Aircraft operations are simulated under three wave height: 0.5 m, 1.0 m, and 1.5 m, with three variations in relative wave direction: 90°, 180°, and 0°, within a wave frequency range of up to 2 rad/s. The simulation of the floater model attempts to predict the vertical bending moment experienced by the structure; this value is subsequently utilized as input in static load modelling through the finite element method to determine the maximum stress value. A probabilistic approach was employed to account for the stochastic characteristics of wave loads, with all potential loads represented as a probability density function (PDF). Moreover, the structural reliability evaluation, which ascertains the likelihood of structural failure, was estimated by combining the load PDF with the strength PDF, derived from CEVL material testing. The evaluation results indicate that the probability of structural failure is -0.34, -0.23 and -0.029 for wave heights of 0.5 m, 1.0 m, and 1.5 m, respectively. The reliability of the floater structure might be enhanced by diminishing the stress induced by wave loads by reinforcement of floater's longitudinal structure and/or the fortification of the CEVL material.

1. Introduction

N219 known as Indonesia aircraft as utility aircraft. This aircraft has 2 twin-engines with 17 until 19-seater, this transport aircraft that designed for multi-purpose missions in remote areas in Indonesia, which is as archipelago country. The N219 can carry loads up to 7,030 kg at take-off and 6,940 kg on landing operation. The operating empty weight of the aircraft (without payload) is 4,039 kg. Type Certificate for N219 aircraft is obtained after flying for 340 hours. The N219 aircraft can fly with a maximum speed of 210 knots, and a lowest speed of up to 59 knots (PTDI, 2022). The urgencies of conversion the aircraft to amphibious as seaplane or floatplane configuration are connecting each island and flexibility of her to landing and take-off not only on land but also in waterfront areas. The conversion will replace wheel on two side below the fuselage with two demi hull floaters. With these reasons, is essential to design and analyze of reliability structure floater itself, especially vertical bending moment that occur when operational of floatplane.

In the context of amphibious conversion, the floater functions as a critical structural component that directly interacts with stochastic wave environments during take-off, landing, and floating operations. Random wave excitation generates vertical bending moments along the longitudinal axis of the floater, which may govern the structural safety of the floatplane. Previous investigations on the N219 floatplane floater have shown that variations in wave height and wave heading significantly influence the magnitude of bending moments and the resulting stress distribution within the structure, with head-sea conditions producing the most critical response. Consequently, a purely deterministic strength assessment is insufficient to represent the inherent uncertainties associated with wave loading and material strength. A structural reliability-based approach, incorporating random wave loading analysis, finite element stress evaluation, and probabilistic assessment using Monte Carlo simulation, provides a more representative framework for evaluating the structural performance and failure probability of the N219 floater under realistic operational conditions (Putro et al., 2025).

In previous studies, the structural reliability of the N219 floatplane floater has been investigated to account for the uncertainties associated with wave-induced loads and material strength. (Meiliana *et al.*, 2025) demonstrated that vertical bending moments generated by random wave excitation significantly affect the reliability index of the floater structure, particularly under adverse sea conditions. Their findings indicate that deterministic stress-based evaluation may overestimate structural safety, as reliability levels can decrease to

critical values even when stresses remain below allowable limits. These results highlight the necessity of incorporating probabilistic reliability analysis in the structural assessment of N219 floatplane floaters to ensure adequate safety margins under realistic operational wave environments.

2. Methodology

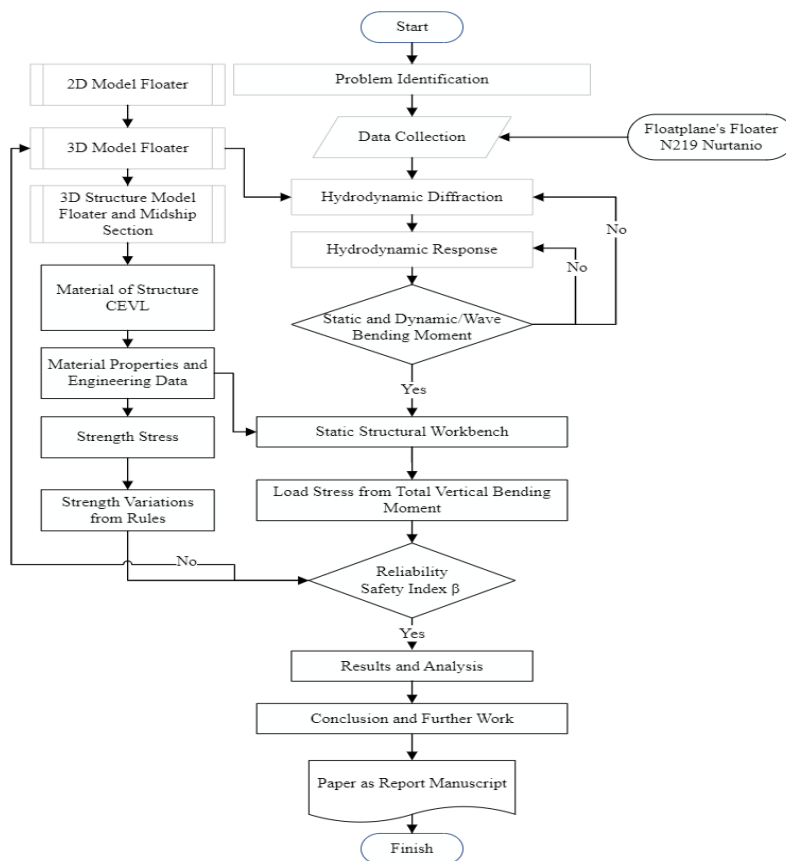


Diagram 1. Flow-Chart of Methodology Study

The research begins with problem identification, focusing on the interaction between ocean waves and the aircraft's floater during waterborne operations. Particular attention is given to the generation of wave-induced loads and their influence on vertical bending moments acting on the floater structure. Following this, a comprehensive data collection stage is conducted. This includes geometric data of the floater, material properties of the structural components, and relevant engineering parameters. A two-dimensional (2D) geometric model is first developed to support preliminary hydrodynamic characterization, followed by a detailed three-dimensional (3D) floater model to accurately represent the actual geometry. In addition, a 3D structural model of the floater and midship section is constructed to enable structural stress analysis and load transfer evaluation.

Material properties of the structure are defined based on certified engineering data and reference standards. These properties include elastic modulus, Poisson's ratio, density, and allowable stress limits, which are essential inputs for the subsequent structural strength assessment. The hydrodynamic analysis is performed through diffraction analysis, which evaluates the interaction between incident waves and the floater body. This analysis yields wave-induced pressures and forces acting on the floater surface. The results are then used in the hydrodynamic response analysis to determine the floater's response characteristics in the frequency domain. These responses form the basis for calculating both static and dynamic wave-induced bending moments.

When the calculated bending moments are found to be significant, the analysis proceeds to the static structural assessment using a static structural workbench. In this stage, the total vertical bending moment, derived from hydrodynamic loading, is applied to the structural model. The resulting stress distribution within the floater structure is evaluated to identify critical regions subjected to maximum stress levels. The computed stresses are then compared against strength criteria derived from applicable design rules and standards. If the stress levels do not satisfy the prescribed limits, structural modifications or reassessments are required.

Conversely, if the criteria are fulfilled, the study advances to the reliability evaluation phase. Structural reliability is assessed through the calculation of the safety index (β), which quantifies the margin between structural capacity and applied loads. This index serves as an indicator of the probability of failure and the overall safety level of the floater structure under wave-induced loading conditions.

Finally, the results are compiled and discussed in the results and analysis section, emphasizing the relationship between hydrodynamic response, structural stress behavior, and safety performance. The study concludes with a summary of key findings and recommendations for future work, and the complete analysis is documented in the form of a scientific report manuscript.

2.1 N219 Floatplane and Floater Lines Plan Configuration

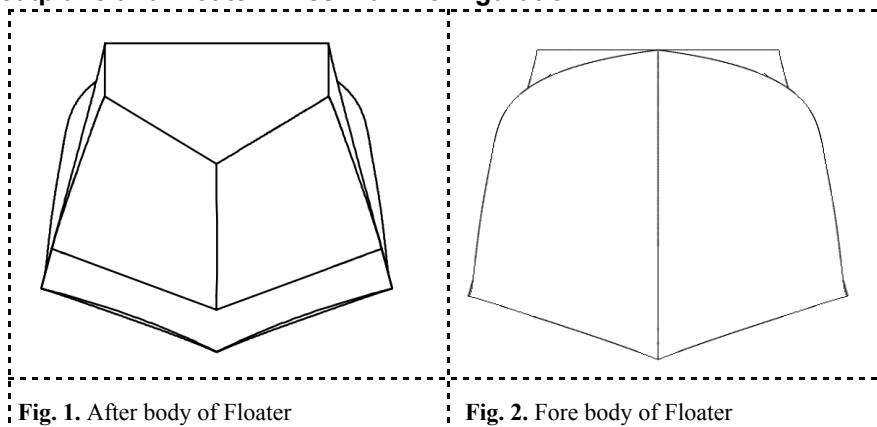


Fig. 1. After body of Floater

Fig. 2. Fore body of Floater

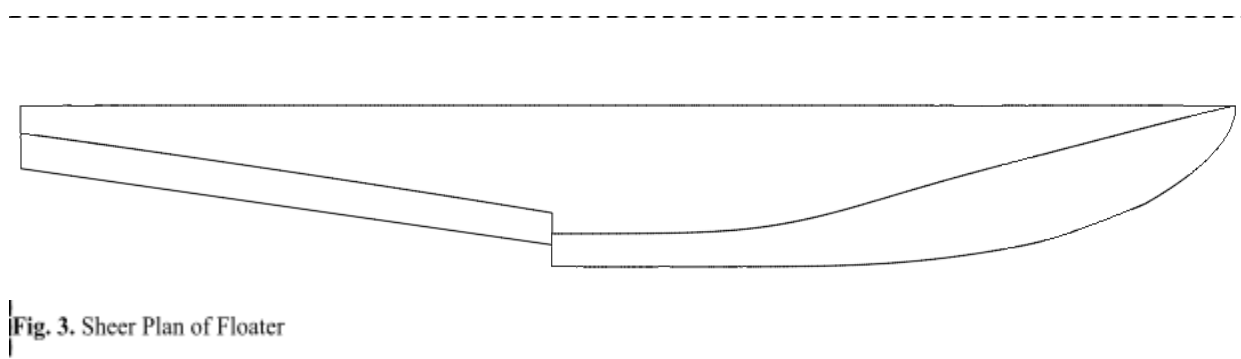


Fig. 3. Sheer Plan of Floater

The design of floater according to (Aliffrananda, 2021) and (Washoya, 2019) used for this study to analyzed the reliability and to design the structural that suitable and reliable during bending moment that applied in operational itself.

Table 1. Main Dimension of Floater

Principal Dimension	Magnitude
Length Overall (LOA)	9.60 m
Length of Waterline (LWL)	9.448 m
Breadth of Demi hull (B)	1.25 m
Height (H)	1.10 m
Draught (T)	0.77 m
Space between demi hull (S)	3.95 m
Forebody length (L_f)	5.4 m
Afterbody length (L_a)	4.2 m

Deadrise angle	20°
Displacement (Δ)	7.330 ton

2.2 Floater Structure and Material

Material used for this study is called Carbon Vinyl Ester Laminate. Known as suitable in application aircraft, coatings, pipes, tanks, windmill blades, carbon vinyl ester laminate (CEVL) with outstanding properties related to chemical and corrosion resistance (Wypych, 2016). Constraints of structural design in floater are weight and strength. The weight of total demi-hull should not exceed the requirement allowed, which is 2.99 ton.

Table 2. Material Properties of CEVL

Material Property	Magnitude	Unit
Density (ρ)	1600	kg/m ³
Young Modulus (E)	55	GPa
Tensile Strength (X_T)	890	MPa
G_{12}	4.5	GPa

Source: (Gargano et al., 2019)

From Table 2, X_T represents the maximum tensile stress that the material can withstand along the primary fibre direction before failure, as for G_{12} represents the material's resistance to shear deformation within the laminate plane, specifically in the plane defined by the fibre direction (1-direction) and the transverse direction (2-direction). Material Properties and engineering data input in static structural workbench for material Carbon-Vinyl Ester Laminate can be seen in Table 3.

Table 3. Material Properties CEVL for Input Calculations

Material Properties CEVL			
Property			unit
Density	ρ	1600	kg/m ³
Young's Modulus	E	55	GPa
Tensile Strength	X_T	890	MPa
Poisson Ratio	ν	0.25	

Table 4. Weight Floater Calculation

Scantling Structure with Carbon Vinyl Ester Laminate CEVL			
Part	area (m ²) or volume (m ³)	Thickness (m)	Weight (ton)
Shell	29.15	0.014	1.30
Bulkhead	2.25	0.012	0.08
Longitudinal	0.011		0.036
	Demi hull	Σ weight (ton)	1.42

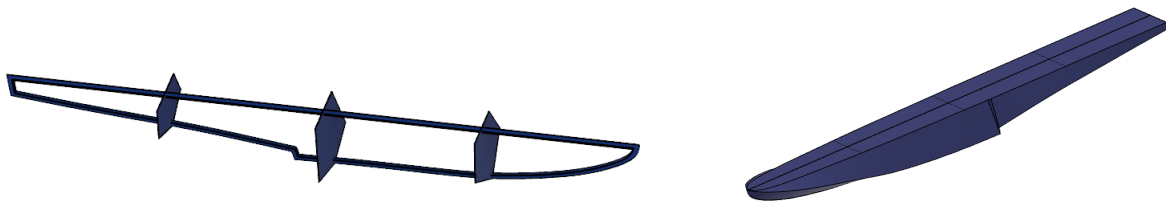


Fig. 4. Bulkhead Configuration Structure and 3D Model Floater

The minimal requirement of watertight compartment that must be in each hull of floater is 4 (four) units. This means each floater should have 3 watertight bulkheads. The calculation of weight estimation of hull structure above with tabulation manually measures volume of scantling times with density of CEVL. With material define as CEVL, Table 5 below detailed scantling that used for structure of floater.

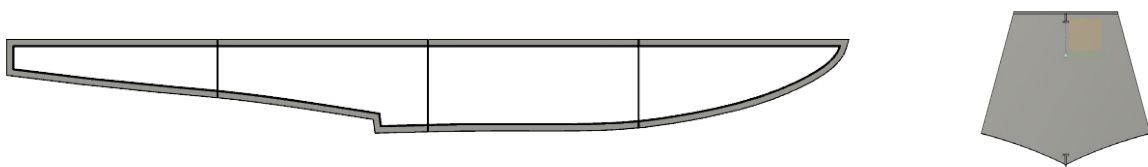


Fig. 5. Bulkhead Arrangement and Midship Section Structure

Table 5. Scantling Floater

Part		Thickness (m)
Shell	Deck	0.014
	Side	0.014
	Bottom	0.014
	Step	0.014
	Transom	0.014
Bulkhead	BHD 1	0.012
	BHD 2	0.012
	BHD 3	0.012
Longitudinal	Web	0.06
	Face	0.04

2.3 Ship Motions

Grid independence conducted to find optimum configuration. With several types of grids or meshing, found optimum configuration as shown in Figure 6. Comparison value of element or mesh size with minimum response in Mesh element size used 0.075 m for Hydrodynamic Diffraction analysis with amount number of element and nodes are 60,959 and 153,725, respectively.

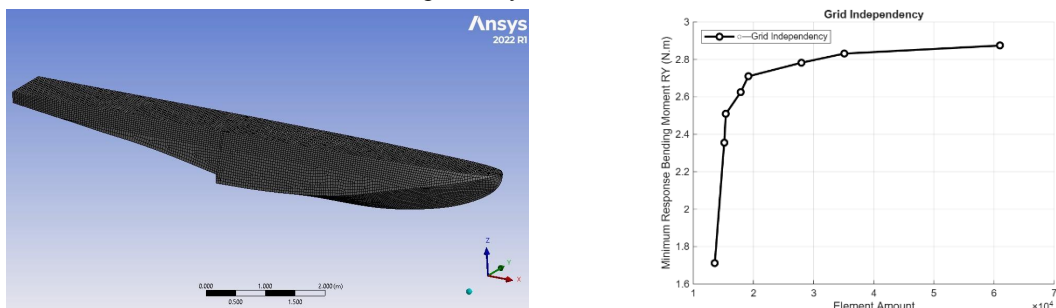


Fig. 6. Mesh model floater Hydrodynamic Diffraction and Grid Independency Study

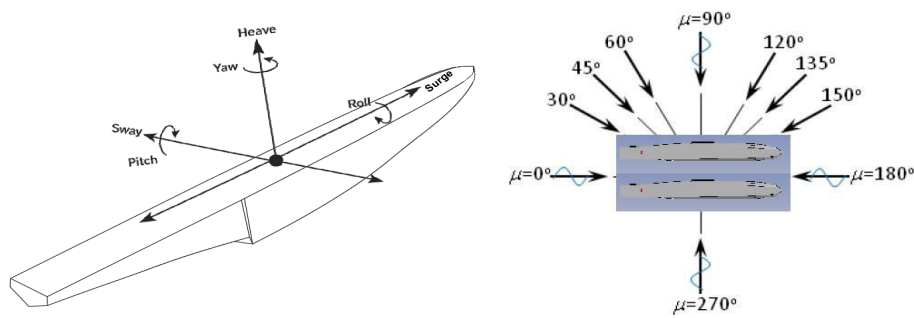


Fig.7. Degrees of Freedom and Wave Direction to Body

Based on Figure 7 shown that degrees of freedom for floating structure and wave direction along of demi hull of floatplane's floater. Ship motion formulation as general defines with formulation of $(M + A(x))\ddot{x} + B(x, \dot{x})\dot{x} + C(x)x = F(x, \dot{x}, t)$. This study analyzed vertical bending moment in floater with 3 wave directions head seas, beam seas and following seas.

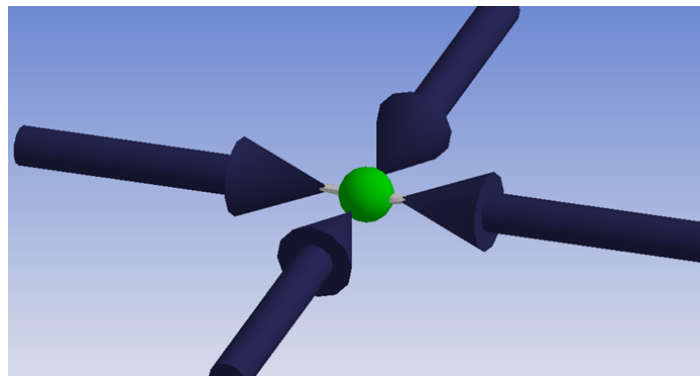


Fig. 8. Wave Direction to Floater

The definition by (Bretschneider, 1959) at about wave spectrum is represents the wave energy (or wave amplitude) distribution of individual wave frequencies in a stationary sea state. Pierson-Moskowitz (PM) known as a type of wave spectra that optimum with 2 parameters.

$$S(\omega) = \frac{5}{16} H_s^2 \frac{\omega_p^4}{\omega^5} \exp \left[-\frac{5}{4} \left(\frac{\omega_p}{\omega} \right)^4 \right]$$

T_p with ITTC definition as the wave or the period of another response like vertical bending moment, in second, with most energy in the wave or response spectrum, i.e. the most probable maximum wave or response in a short-term sea state. The wave frequency for ω with unit rad/s and ω_p define as spectral peak frequency in rad/s. With this parameter, this research used the formulation of Pierson-Moskowitz's formula as below:

$$S(\omega) = \frac{1}{2\pi} \frac{H_s^2}{4} \left(\frac{2\pi}{T_z} \right)^4 \omega^{-5} \exp \left[-\left(\frac{2\pi}{T_z} \right)^4 \omega^{-4} \right]$$

Where $S(\omega)$ is Pierson-Moskovitz spectrum ($m^2/(rad/s)$), H_s known as significant wave height, and T_z as average zero up-crossing wave period (s), also ω wave frequency (rad/s). From plot of graphics results shown in Figure 9 which range of wave frequency (rad/s) that implied significant value for spectral energy. There were 4 range of frequency, 0.1 to 1.0, 1.0 to 2.0, 2.0 to 3.0 to 4.0. Frequency of wave 0.1 until 1.0 observed give significant value for H_s 0.5 m, with range 0.4 1.2 for H_s 1.0 m. This study analyzed and found from 0.1 until 2.0 rad/s for significant range period in hydrodynamic response analysis.

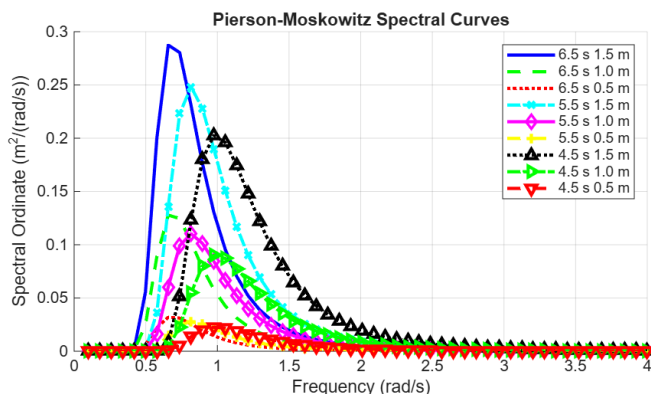


Fig. 9. Spectrum Wave for Significant Wave (H_s) variations

This study conducted for area of java seas. The java seas have surface area of the sea is 320,000 square kilometers and the average depth is 46 m. The maximum length and maximum width of the sea are 1600 km and 380 km respectively. The average depth of the sea is just 46 meters because it is a shallow sea as shown in Figure 10 (The Editors of Encyclopedia Britannica, 2019).

The analysis attended to several values of H_s and peak period T_z that have value more than 500 for the probabilities. This wave scatter diagram as seen in Table 6, consists of several cells. Each cell of wave scatter diagram which are short-term descriptions of the sea in terms of joint probability of occurrence of a significant wave height H_s and a characteristic period. These cells contain 3 minimum data items below:

- a. The significant wave height H_s (usually in meter),
- b. The characteristic wave period (in seconds),
- c. The number of occurrences for the sea state.

Table 6. Wave scatter Diagram of Java Sea

H_s (m)	Wave Periods (s)													Sum
	3.5	4.5	5.5	6.5	7.5	8.5	9.5	10.5	11.5	12.5	13.5	14.5	15.5	
0.5	94	321	161	11	19	14	7	5	4	2	1			639
1	22	119	138	712	316	285	16	89	57	27	8	3	1	4476
1.5		185	680	408	527	213	16	120	67	31	11	5	2	2411
2			71	229	404	323	66	37	34	19	10	9	2	1204
2.5				33	185	290	86	20	12	7	2	2	1	638
3				1	33	218	97	10	4	2			1	366
3.5					1	60	81	8	1	1				152
4						7	45	10	1					63
4.5							20	16	1					37
5							2	7	1					10
5.5								3	1					4

Sum	321	1703	2300	1394	1485	1410	732	325	183	89	32	19	7	10000
------------	-----	------	------	------	------	------	-----	-----	-----	----	----	----	---	-------

Source: (Wibowo, 2012; Kadhafi, 2016)

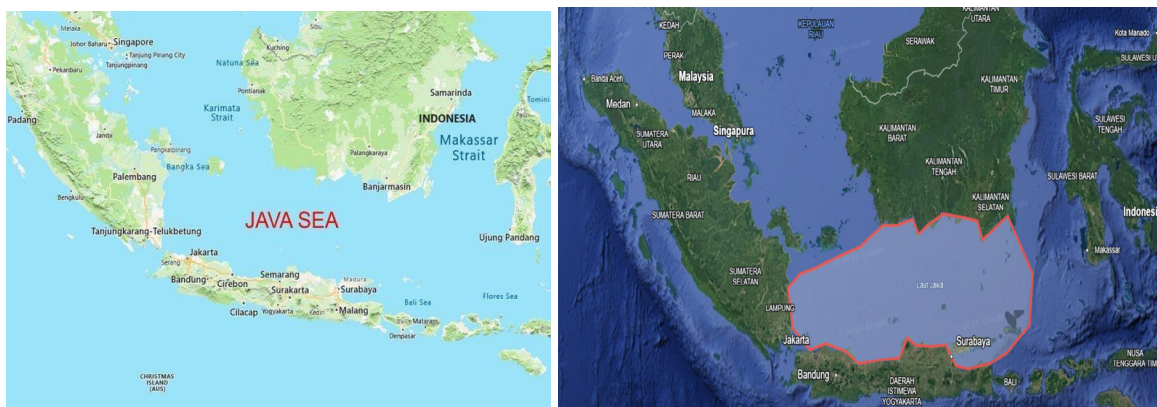


Fig. 10. Java Seas in Map

Source: (The Editors of Encyclopedia Britannica, 2019)

The peak period should be defined for calculated in Hydrodynamic response. The range of significant frequency starts from 0.1 to finish frequency 2.0 rad/s with T_z are 4.5 s, 5.5 s and 6.5 s. From Table 7, the value of periods that are used for zero up-crossing period in wave. The calculation with wave direction 0° , 90° , and 180° and forward speed of floater used 9.625 m/s each T_z and wave directions, this study calculated for bending moment static and dynamic has been done with several results. As explained for static vertical bending moment, conducted calculations for RY components in ANSYS AQWA TM. After Statical Bending Moment found, Dynamic Bending Moment used the workbench Hydrodynamic Diffractions, which got several values for each variation shown in Figure 12, Figure 13 and Figure 14.

Table 7. Wave Periods and its Frequencies from Java Seas Wave Scatter

Hs(m)	Wave Periods (s)			Sum
	4.5	5.5	6.5	
0.5	321	161	11	493
1.0	1197	1388	712	3297
1.5	185	680	408	1273
Sum	1703	2229	1131	5063

Hs (m)	Frequencies (rad/s)			Sum
	1.39	1.14	0.96	
0.5	321	161	11	493
1.0	1197	1388	712	3297
1.5	185	680	408	1273
Sum	1703	2229	1131	5063

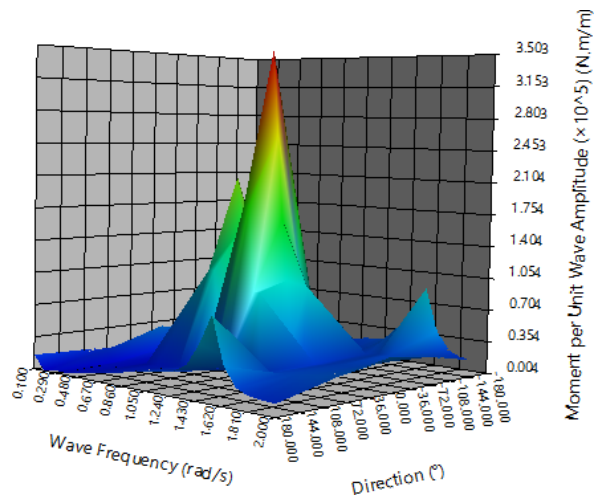


Fig. 11. Typical of Bending Moment (RAO) for RY Vertical

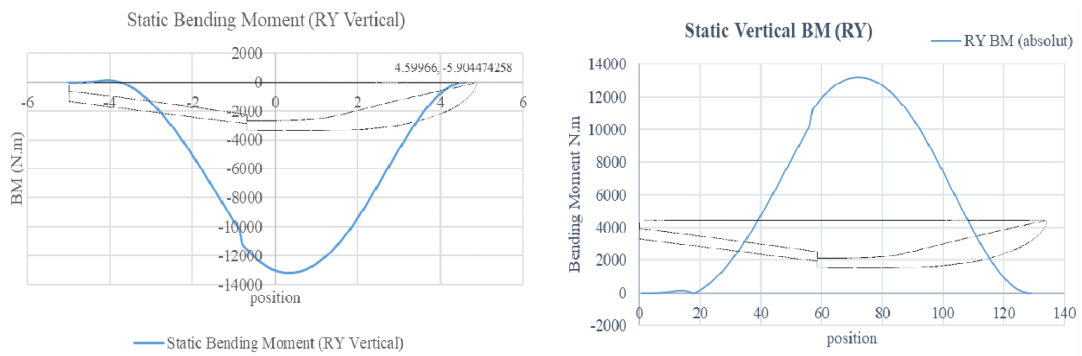
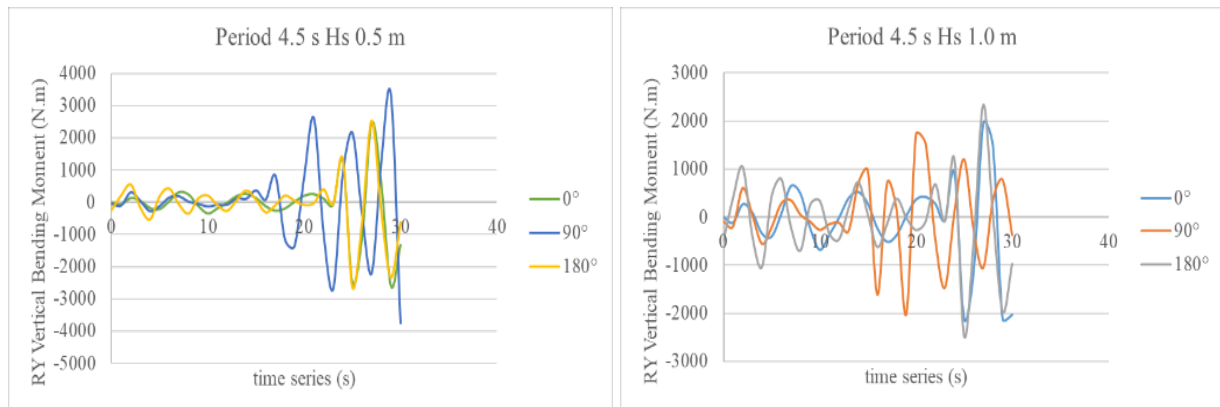


Fig. 12. Static Bending Moment Floater for Vertical Bending Moment (RY)



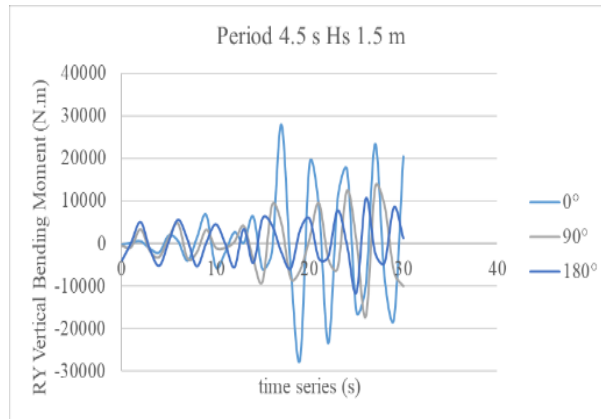


Fig. 13. Dynamic Vertical Bending Moment Hs 0.5 m

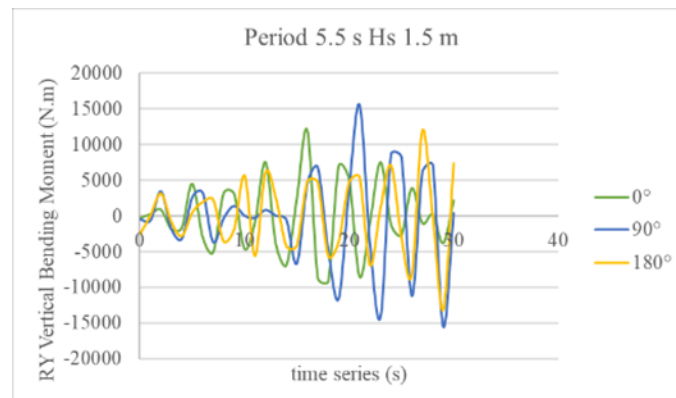
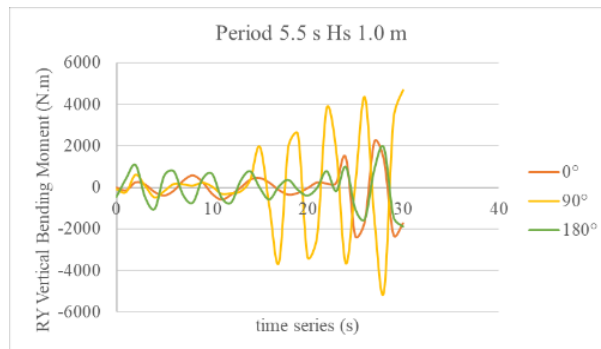
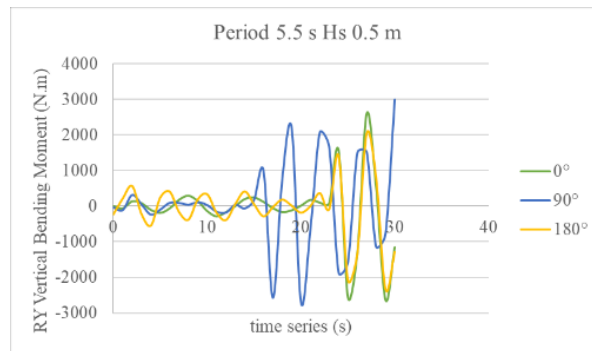


Fig. 14. Dynamic Vertical Bending Moment Hs 1.0 m

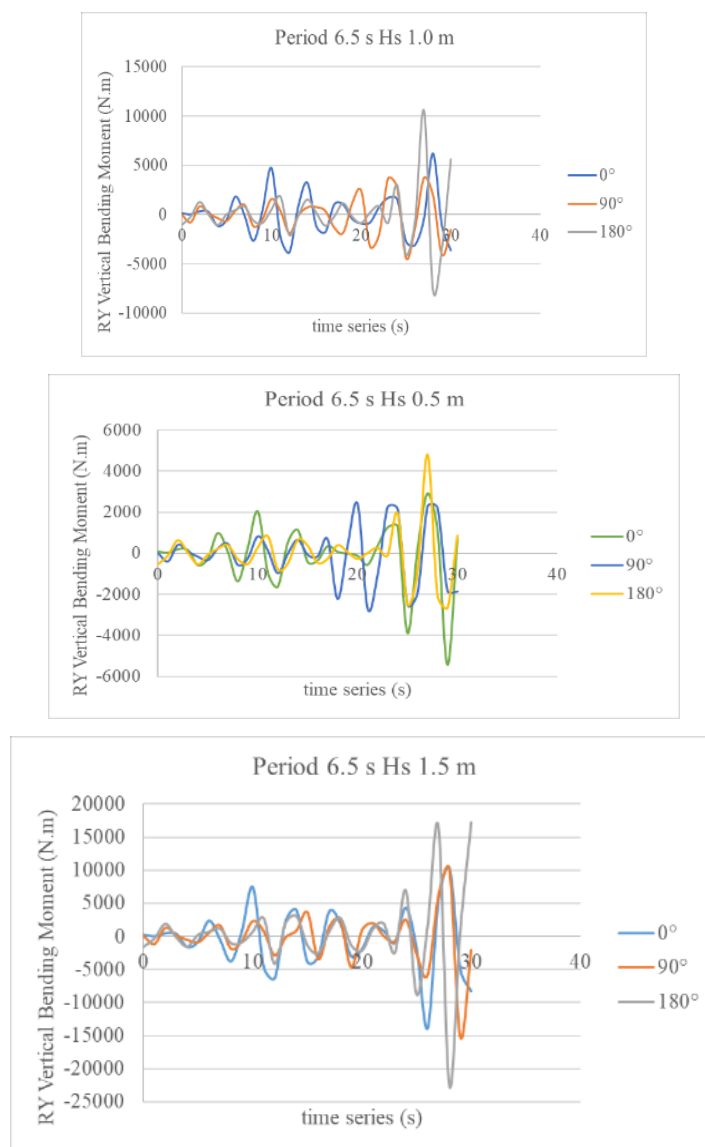


Fig. 15. Dynamic Vertical Bending Moment Hs 1.5 m

2.4 Structural Stress Analysis

Structural stress analysis is performed to quantify the stress response of the amphibious aircraft floater under wave-induced loading conditions. The analysis is conducted using the Finite Element Method (FEM), which is widely applied in marine and offshore structural engineering for evaluating the response of floating structures subjected to hydrodynamic loads. The adopted methodology follows established practices recommended by the Ship Structure Committee (SSC) for global structural strength assessment under wave excitation.

Wave-induced loads acting on the floater are obtained from time-domain hydrodynamic simulations using ANSYS AQWA. The hydrodynamic response is expressed in terms of vertical bending moment, which represents the dominant global load component affecting the longitudinal strength of floating structures. According to SSC guidelines, global wave loads may be transferred to the structural model in the form of equivalent bending moments when assessing overall structural response.

The structural analysis is performed using a quasi-static FEM approach, assuming that the wave encounter frequencies are significantly lower than the natural frequencies of the floater structure. Under this assumption, dynamic amplification effects are considered negligible, and the structural response is governed primarily by static equilibrium. This approach is commonly applied in wave-induced structural analyses of ships and floating bodies and provides an efficient and sufficiently accurate representation of global stress behavior.

The floater structure is discretized into finite elements connected at nodal points, forming a numerical model capable of capturing global deformation and stress distribution. The governing equilibrium equation of the FEM formulation is expressed as:

$$Ku = F$$

where K denotes the global stiffness matrix, u is the nodal displacement vector, and F represents the external load vector derived from the applied vertical bending moment. Material properties and geometric characteristics of the floater are incorporated into the stiffness formulation.

The displacement field obtained from the FEM solution is used to compute strain and stress distributions within the structure based on linear elastic constitutive relations. The structural stress response is evaluated using the von Mises equivalent stress, which is adopted as the representative stress parameter for assessing structural performance. Stress evaluation is focused on longitudinal structural components, as these members primarily resist global bending loads induced by wave action.

Considering the stochastic nature of wave excitation, the resulting structural stress is treated as a random variable. The probabilistic distribution of stress is obtained by propagating the wave load probability density function through the FEM-based structural response model. This procedure ensures that the variability of the wave environment is reflected in the structural stress response.

Structural reliability is assessed by combining the stress probability density function with the material strength probability density function obtained from CEVL material testing. Failure is defined using a limit state function:

$$g(R, S) = R - S$$

where R represents material resistance and S denotes applied structural stress. Structural failure is assumed to occur when $g(R, S) < 0$. The probability of failure is determined by evaluating the overlap between the stress and strength distributions for each wave condition.

The adopted structural stress analysis framework provides a consistent basis for evaluating the reliability of amphibious aircraft floaters operating in stochastic wave environments. The results indicate that structural reliability may be improved through reduction of wave-induced stress, particularly by reinforcing longitudinal structural members and enhancing material strength, in accordance with SSC-based structural design recommendations.

2.5 Load Stress Calculation

The analysis of stress that floating body experiences could be several types combinations of load, but in this study only analyzed about vertical bending moment. By definition of about bending moment define as R or rotation component in AQWA™ (Manual Aqwa 14.5, n.d.). This study conducted only vertical bending moments from coupled motions heave and pitch. From data static and dynamic bending moment, applied in static structural workbench to found and calculated for bending moment total (MT).

Table 8. Vertical Bending Moment

Variation	Wave Period (s)	Wave Height (m)	Wave Directions (°)	Ms Static (N.m)	Mw Wave or Dynamic (N.m)	MT Total (N.m)
V1	4.5	0.5	Following Seas 0°	13201.10	2585.67	15780.78
V2			Beam Seas 90°		3755.42	16956.53
V3			Head Seas 180°		2045.05	15840.14
V4		1.0	Following Seas 0°		2110.30	15311.40
V5			Beam Seas 90°		2017.14	15218.25

Variation	Wave Period (s)	Wave Height (m)	Wave Directions (°)	Ms Static (N.m)	Mw Wave or Dynamic (N.m)	MT Total (N.m)		
V6			Head Seas 180°		2474.99	15676.09		
V7		1.5	Following Seas 0°		28091.93	41293.04		
V8			Beam Seas 90°		17160.94	30362.05		
V9			Head Seas 180°		11589.88	24790.99		
V10	5.5	0.5	Following Seas 0°		2637.71	15838.81		
V11				Beam Seas 90°		2987.92	16189.03	
V12				Head Seas 180°		2320.70	15521.80	
V13			1.0	Following Seas 0°		2335.98	15537.08	
V14				Beam Seas 90°		5024.60	18225.71	
V15				Head Seas 180°		1906.92	15108.03	
V16			1.5	Following Seas 0°		11986.41	25187.52	
V17				Beam Seas 90°		15495.11	28696.22	
V18				Head Seas 180°		13185.63	26386.74	
V19		6.5	0.5	Following Seas 0°		5442.77	18643.87	
V20					Beam Seas 90°		2681.49	15882.60
V21					Head Seas 180°		4825.26	18026.37
V22			1.0	Following Seas 0°		6203.50	19404.61	
V23				Beam Seas 90°		4424.65	17625.76	
V24				Head Seas 180°		10543.95	23745.06	
V25			1.5	Following Seas 0°		13853.17	27054.28	
V26				Beam Seas 90°		15199.5	28400.65	
V27				Head Seas 180°		22654.03	35855.14	

Remoted displacement at 3 points used for calculated and analyzed in workbench as boundary condition. With several load and moment with remoted displacement applied as boundary conditions, stress value found for every variation of case. From Table 8 above applied to static structural as moment at 2 position AP and FP from bending moment total each variation with several value static or constant:

- a. Hydrostatic Load with value generated by workbench,
- b. Load Body with value as weight load from mass displacement of floater type found 35953.65 N with gravitational acceleration 9.81 m/s²,
- c. Remoted Displacement for boundary conditions.

From static structural workbench analysis, found that distribution of load stress accumulation centralized in area transitional along from forebody to after body. Another area is simply evaluated as evenly distributed from stress distributions. From vertical bending moments and other loads that applied in through floater structure, shown in Figure 18 that deformation and stress highly occurred in area of stepped plate with bottom stringer and bottom plate near it.

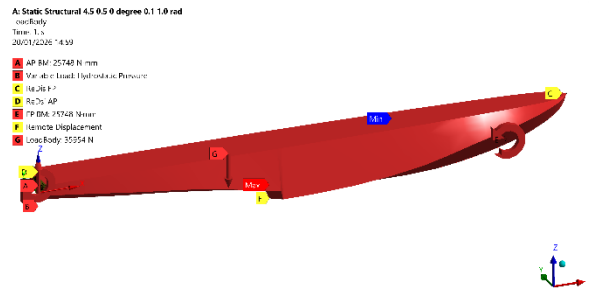
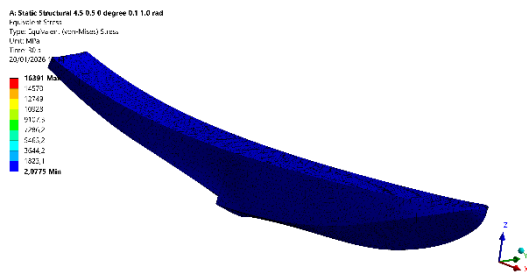
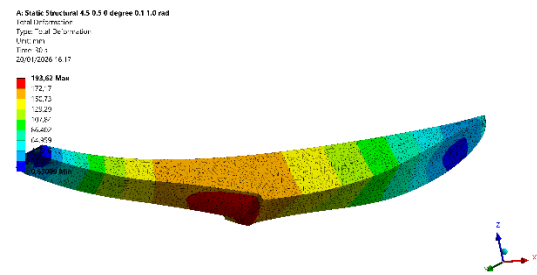


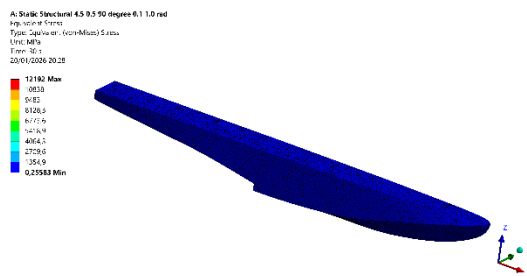
Fig. 16. AP and FP Bending Moment Applied with Hydrostatic Pressure Load and Load Body Applied in Static Structural as Boundary Condition



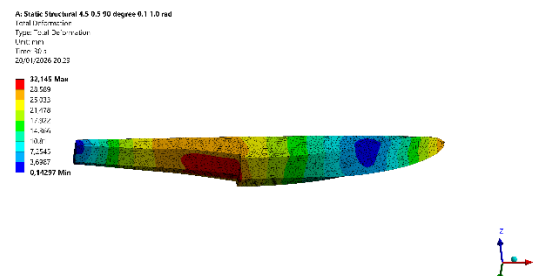
Stress in period 4.5 s and Hs 0.5 m of head seas



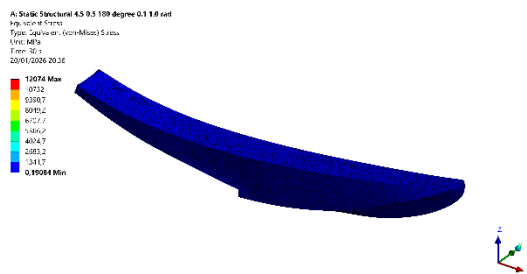
Deformation in period 4.5 s and Hs 0.5 m of head seas



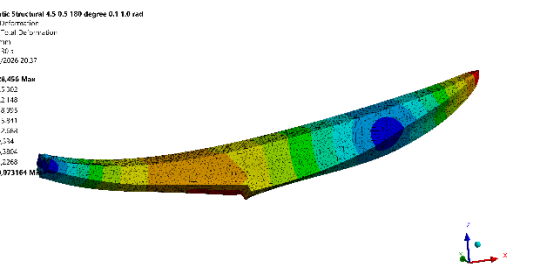
Stress in period 4.5 s and Hs 1.0 m of beam seas



Deformation in period 4.5 s and Hs 1.0 m of beam seas



Stress in period 4.5 s and Hs 1.5 m of following seas



Deformation in period 4.5 s and Hs 1.5 m following seas

Fig. 17. Load Stress and Deformation Results Calculation in Static Structural

2.6 Assessment Safety Index (β) for Material Structure

For the strength of stress structure has define with reductions factor by (Biro Kasifikasi Indonesia BKI, 2021) as shown in Table 9. With the regulation and recommendation or guidelines from (Biro Klasifikasi Indonesia BKI, 2021), this study calculate and stated for variation reduction in tensile strength of structure with CEVL material shown in Table 10. Probability density function from value of variations CEVL used for strength analysis shown in Figure19. Based on the BKI *Rules For Classification and Construction*, the allowable variations for fibre-reinforced composite materials can be summarized as follows:

$$\sigma_{perm} = \frac{R_m \cdot R_1 \cdot R_2 \cdot R_3 \cdot R_8}{S} [N/mm^2]$$

Table 9. Reduction Factor for Laminates

Reduction Factor Description	Symbol	Value / Limitation
Statistical long-term loading (sea loads)	(R ₁)	(< 0.75)
Static long-term loading (tank walls)	(R ₂)	(< 0.50)
Raised temperature	(R ₃)	(< 0.90)
Ageing	(R ₄)	(< 0.80)
Manufacturing (hand lay-up)	(R ₅)	(= 0.90)
Manufacturing (prepreg)	(R ₅)	(= 1.00)
Fatigue, (N < 10 ²)	(R ₆)	(= 1.00)
Fatigue, (N < 10 ³)	(R ₆)	(= 0.80)
Fatigue, (N < 10 ⁶)	(R ₆)	(= 0.40)
Different material properties	(R ₇)	(< 0.90)
Moisture	(R ₈)	(< 0.80)

Table 10. Variations Reduction for Material CEVL

N O	Reduction for Laminated	Symb ol	σ _{perm}	σ _{perm}	σ _{perm}	σ _{perm}	σ _{perm}	σ _{perm}	σ _{perm}	σ _{perm}	σ _{perm}	σ _{perm}	σ _{perm}	σ _{perm}
			A	B	C	D	E	F	G	H	I	J	K	L
1	Statical long-term loading (sea loads)	R ₁ < 0.75	0.7	0.70	0.70	0.70	0.70	0.70	0.70	0.70	0.70	0.70	0.70	0.70
2	Static-long term loading (wall tanks)	R ₂ < 0.5	0.45	0.45	0.45	0.45	0.45	0.45	0.45	0.45	0.45	0.45	0.45	0.45
3	Raised temperature	R ₃ < 0.9	0.85	0.85	0.85	0.85	0.85	0.85	0.85	0.85	0.85	0.85	0.85	0.85
4	Ageing	R ₄ < 0.8	0.75	0.75	0.75	0.75	0.75	0.75	0.75	0.75	0.75	0.75	0.75	0.75
5	Manufacturing i.e.:													
	- Hand Lay-up	R ₅ = 0.9	1.00	1.00	1.00	0.90	0.90	0.90	0.85	0.85	0.85	0.77	0.77	0.77
	- Prepeg (human error)	R ₅ = 1.0												
6	Fatigue N load:													
	N < 10 ²	R ₆ = 1.0	1.00	0.80	0.40	1.00	0.80	0.40	1.00	0.80	0.40	1.00	0.80	0.40
	N < 10 ³	R ₆ = 0.8												
	N < 10 ⁶	R ₆ = 0.4												
7	Different material properties	R ₇ < 0.9	0.85	0.85	0.85	0.85	0.85	0.85	0.85	0.85	0.85	0.85	0.85	0.85
8	Moisture	R ₈ < 0.8	0.75	0.75	0.75	0.75	0.75	0.75	0.75	0.75	0.75	0.75	0.75	0.75
	Strength		103.578	82.863	41.431	93.220	74.576	37.288	88.041	70.433	35.217	79.237	63.390	31.695

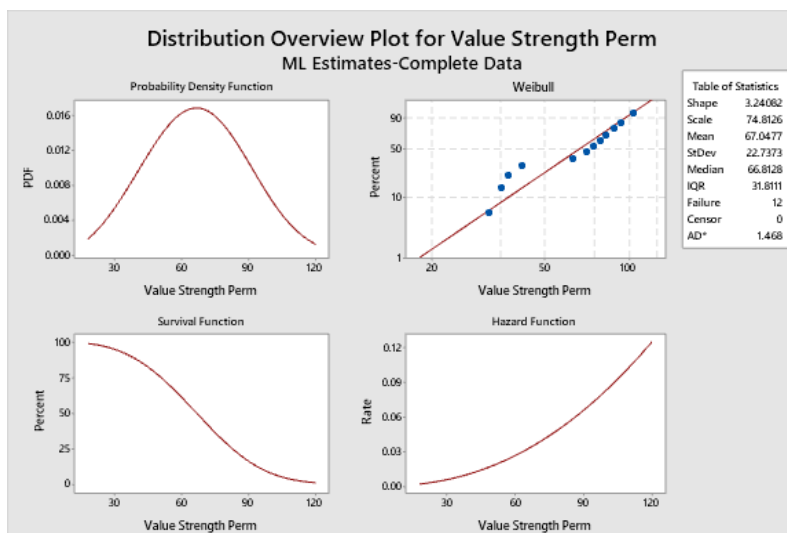


Fig. 18. Distribution of Strength of Stress Material CEVL for Structure Floater

3. Result and Analysis

With several steps of analyses in this study, to found strength stress and load stress data from design, Hydrodynamic Diffraction, Hydrodynamic Response until Static Structural as workbench analyses in ANSYS™, in this stage conducted analysis for reliability. Reliability itself define as is its ability to fulfil its design purpose for some specified reference period (Thoft-Christensen & Murotsu, 1986). Most structures have a number of possible failure modes. Therefore, in determining the reliability of a structure this fact must be taken into account (Daniel Mohammad Rosyid, 2007). The first step will usually be to estimate the structural reliability with respect to each specified failure mode, i.e. the probability that the structure will not attain each specified failure mode (ultimate or serviceability) during the specified reference period.

$$\beta = \frac{\mu_s - \mu_z}{\sqrt{\sigma_s^2 + \sigma_z^2}}$$

$$P_f = 1 - \beta$$

Based on (Ship Structure Committee SSC, 1990) the definitions of μ_s , μ_z as mean of strength stress and load stress, respectively, and σ_s , σ_z as standard deviations of strength stress and load stress also, respectively. The reliability index (β) and probability of failure (P_f) calculated with formulation above with each results give in Table 11. From Table 11 and Table 12, could be explained for safety index from variations of H_s and wave directions. The two tables had values for μ and σ as mean value and standard deviation and calculated for safety index and probability failure. With several of withdrawn results that shown in Figure 20 and Figure 21, typically the type of the strength distribution followed by the load distribution, with formula below for gaussian S and normal distribution formula of probability density function.

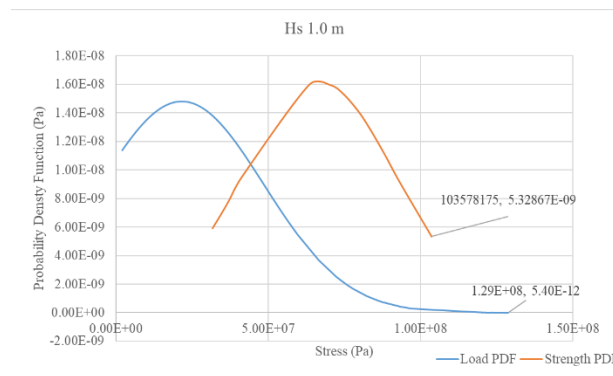
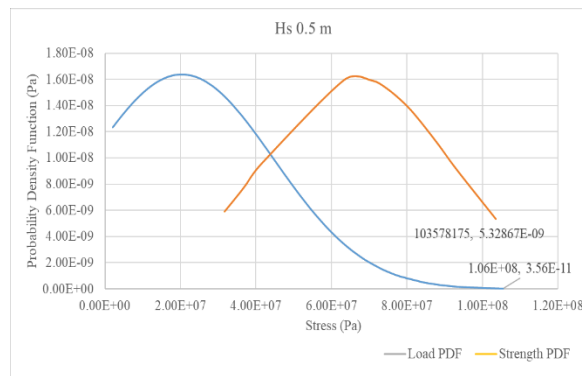
$$PDF(x) = \frac{1}{\sigma\sqrt{2\pi}} e^{-x^2/2\sigma^2}$$

Table 11. Recapitulation of Safety Index and Probability Failure for Hs Variations

Strength [S]		Load [Z]			
		Hs 0.5 m	Hs 1.0 m	Hs 1.5 m	
μS	6.67×10^7	μz	2.03×10^7	2.16×10^7	2.54×10^7
σS	2.48×10^7	σz	2.43×10^7	2.70×10^7	3.16×10^7
		β	1.34	1.23	1.03
		P(f)	-0.34	-0.23	-0.03

Table 12. Recapitulation of Safety Index and Probability Failure for Wave Direction Variations

Strength [S]		Load [Z]			
		0°	90°	180°	
μS	6.67×10^7	μz	1.76×10^7	3.12×10^7	1.88×10^7
σS	2.48×10^7	σz	2.46×10^7	3.23×10^7	2.38×10^7
		β	1.41	0.87	1.39
		P(f)	-0.41	0.13	-0.39



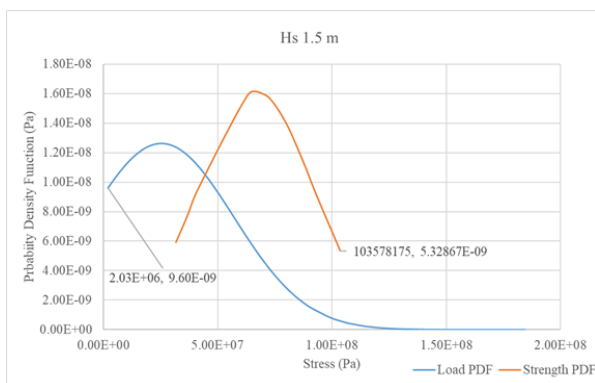


Fig. 19. Probability Density Function for each Hs variations

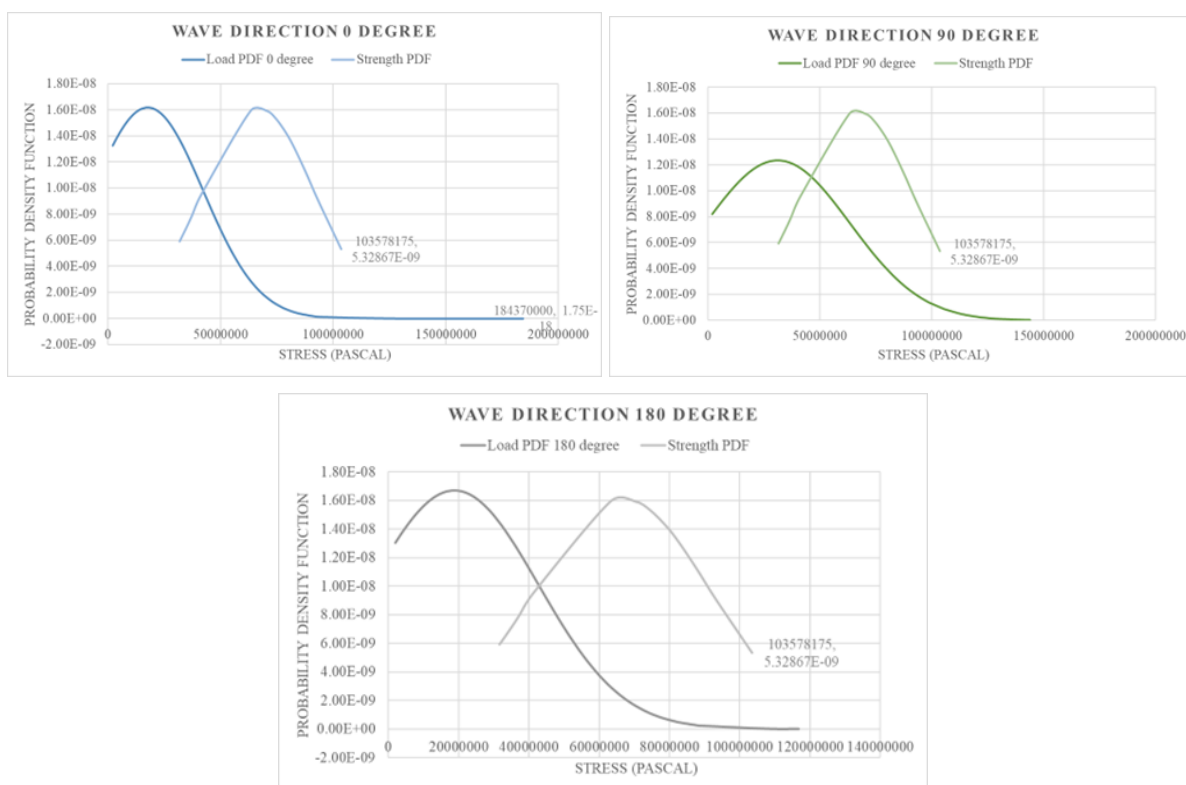


Fig. 20. Probability Density Function for each Wave Directions variations

4. Conclusion

From this study found that higher of significant wave height (H_s) give lower safety index (β), highest significant height ($H_s = 1.5$ m) gave lowest safety index $\beta = 1.03$. In detail wave direction gave lowest safety index is 90 degree or beam seas with values 0.87. The reliability and failure analysis indicates that the forebody–afterbody transition region requires increased material stiffness and/or larger scantling dimensions, as reflected by the decreasing reliability index ($\beta = 1.34–1.03$) and the corresponding increase in failure probability under higher wave conditions. Finally, this simply method of reliability safety index could use for analyzing reliability of body/hull of floatplane’s floater N219 from vertical bending moment.

Acknowledgement

The Authors highly appreciated for Department of Naval Architecture ITS for providing research facilities supporting this research.

References

- Aliffrananda, M. H. N. (2021). *Studi Ketidakstabilan Porpoising pada Floatplane dalam Operasi Lepas Landas di Perairan Tenang* [Master Thesis]. Institut Teknologi Sepuluh Nopember Surabaya.
- Biro Klasifikasi Indonesia BKI. (2021). *Rules For Classification and Construction*. www.bki.co.id
- Gargano, A., Das, R., & Mouritz, A. P. (2019). *Finite element modelling of the explosive blast response of carbon fibre-polymer laminates*. *Composites Part B: Engineering*, 177. <https://doi.org/10.1016/j.compositesb.2019.107412>
- Muammar Kadhafi. (2016). *Analisis Umur Kelelahan (Fatigue Life) Konstruksi Kapal Perang Tipe Corvett di Perairan Indonesia* [Master Thesis]. Institut Teknologi Sepuluh Nopember ITS.
- PTDI. (2022). N219 Nurtanio. PT Dirgantara Indonesia (Persero). Ship Structure Comitte SSC. (1990). *SSC-351 An Introduction to Structural Reliability Theory*.
- The Editors of Encyclopaedia Britannica. (2019, March 5). "Java Sea." *Encyclopedia Britannica*. <https://www.Britannica.Com/Place/Java-Sea>.
- Thoft-Christensen, P., & Murotsu, Y. (1986). *Application of Structural Systems Reliability Theory. In Application of Structural Systems Reliability Theory*. Springer Berlin Heidelberg. <https://doi.org/10.1007/978-3-642-82764-8>
- Washoya, Z. A. (2019). *Analisis Beban Impact Dengan Variasi Sudut Deadrise Pada Floats Pesawat Amfibi Pada Saat Mendarat Dengan Simulasi CFD* [Undergraduate Thesis]. Institut Teknologi Sepuluh Nopember Surabaya ITS.
- Wypych, G. (2016). VE vinyl ester resin. *Handbook of Polymers*, 702–703. <https://doi.org/10.1016/B978-1-895198-92-8.50214-7>
- Bretschneider, C. L. (1959). *Wave variability and wave spectra for wind-generated gravity waves*. U.S. Army Corps of Engineers.
- ITTC – Recommended Procedures and Guidelines (Seakeeping), 2011.
- Putro B. H., Rochmad A. N., Alifia W. U., Meiliana S. W. & Sulisetyono A. 2025 *Structural reliability study of the N219 floatplane's floater due to random wave loads* IOP Conference Series: Earth and Environmental Science 1473 012032 <https://doi.org/10.1088/1755-1315/1473/1/012032>
- Meiliana S. W., Sulisetyono A. & Alifia W. U. 2025 *Reliability assessment of the N219 floatplane floater under irregular wave loading* Journal of Physics: Conference Series 3132 012015 <https://doi.org/10.1088/1742-6596/3132/1/012015>